Theses and Dissertations

12-2014

Development of a Novel Device for the Perfusion Driven Decellularization of Skeletal Muscle

Benjamin Kasukonis
University of Arkansas, Fayetteville

Development of a Novel Device for the Perfusion Driven
Decellularization of Skeletal Muscle

Development of a Novel Device for the Perfusion Driven
Decellularization of Skeletal Muscle

A thesis submitted in partial fulfillment
of the requirements for the degree of
Master of Science in Biomedical Engineering

by

Benjamin Kasukonis
University of Wisconsin – Stevens Point
Bachelor of Science in Biology, 2005

December 2014
University of Arkansas

This thesis is approved for recommendation to the Graduate Council.

_____

Dr. Jeffrey Wolchok
Thesis Director

_____   _____

Dr. Timothy Muldoon   Dr. Tyrone Washington
Committee Member   Committee Member

ABSTRACT

Decellularization of skeletal muscle is a process that removes cellular components of skeletal muscle tissue while leaving behind the intact extracellular matrix (ECM). Skeletal muscle ECM is currently being studied as a biologic scaffold for repairing volumetric muscle loss (VML) because the removal of cells greatly reduces the antigenicity of the donor tissue. Decellularization usually relies on passive diffusion of detergents, surfactants and/or osmotic solutions to strip cells from the ECM. However, passive diffusion alone is usually not sufficient for complete removal of cells from the interior of large pieces of skeletal muscle using detergents, such as sodium dodecyl sulfate (SDS). The goal of this study was to develop a device that not only removes cells by perfusion from the interior of skeletal muscle, but also monitors the progress of decellularization in real-time. The device, based around a Raspberry Pi, is a stand-alone system that does not require a desktop computer or expensive software packages. Different flow rates (0.1, 1.0 and 10 mL/hr) along with different concentrations of SDS (0.2% and 1.0%) were tested. Decellularization progress was monitored and logged to an online spreadsheet. The device was found to be capable of decellularizing the medial gastrocnemius of a rat in under 10 hours. Complete decellularization was validated using fluorescent imaging. Perfusion decellularized muscle samples were found to have no significant differences in collagen or sulfated glycosaminoglycan (sGAG) content when compared to samples that were decellularized using current passive diffusion protocols. The ECM obtained through the use of this device is currently being used for the repair of VML in a rat model.

Key words: Skeletal muscle, Decellularization, Extracellular matrix, Novel device

TABLE OF CONTENTS

INTRODUCTION

The human body is capable of repairing mild to moderate skeletal muscle

damage. However, these innate repair mechanisms are not able to repair and

regenerate large scale volumetric muscle loss (VML)[1]. Advances in tissue engineering

have yielded researchers and physicians a number of treatment options for other

tissues such as bone and skin[2-4]. In contrast, very few options exist for skeletal muscle

repair, although a number of scaffold-based and cell-based strategies are currently

being developed[3,5,6]. Biologic and synthetic scaffolds have been produced to provide a

stable environment for cell proliferation and the production of contractile tissue in vitro

and in vivo. Corona *et al.* found that a combination of muscle derived cells on an

acellular scaffold provided the most functional recovery compared to an acellular

scaffold alone[7].

Scaffolds that are designed for skeletal muscle tissue engineering are not unlike

scaffolds used for other applications in the body. They must promote the adhesion and

proliferation of cells and must provide the engineered tissue with properties similar to

native tissue. Scaffold integration with host vascular and nervous networks must take

place for successful regeneration of skeletal muscle[6]. Scaffold-based strategies

composed of a biologic or synthetic biomaterial which may or may not be seeded with

cells prior to implantation. Biologic scaffolds include acellular extracellular matrix

(ECM)[7-14],which are derived through the process of decellularization.

Decellularization is a process which removes the cellular components from a

tissue leaving behind the intact ECM[15]. Decellularized tissue is promising as a biologic

scaffold because it retains the biochemical and morphological structure of the native ECM while having dramatically lower antigenicity than an allograft because it lacks foreign cell antigens[15]. Decellularization of tissues and whole organs can be accomplished through the use of chemical agents such as: surfactants, detergents or osmotic solutions[8,15]. Decellularization has been used to produce whole organ scaffolds for the heart[16], liver[17], lungs[18] and kidneys[19]. Whole organ decellularization in many cases has been achieved through the use of vascular perfusion[16-19]. The major inlets and outlets (arteries and veins) and the capillary network of organs allow for perfusion of the entire organ. Skeletal muscle tissue lacks the major arteries and veins that are found in whole organs such as the kidneys, heart and liver. Therefore perfusion decellularization of skeletal muscle will require the introduction of an inlet port into the tissue. Scaffolds composed of decellularized muscle are unique because they retain the parallel alignment of the native muscle from which they were obtained and pores for cell attachment left by the previous cells[9]. Decellularized muscle lacks the antigenicity of an allogenic transplant but requires the infiltration of host cells, innervation, and revascularization with associated integration into the host vasculature to produce functioning myofibers[6,20].

One detergent that has been used extensively in decellularization is sodium dodecyl sulfate(SDS). SDS is an anionic surfactant that removes cells by disrupting the phospholipid bilayer of the cell membrane[15]. Once a cell is lysed, SDS denatures proteins within the cells which allows for more complete removal of cellular components[15]. SDS has been used to decellularize whole organs and tissues for use in tissue engineering applications, including skeletal muscle[11]. In addition, SDS was used

to successfully decellularize whole organs using a perfusion based method. Although SDS has been shown to cause more ECM degradation than other detergents, studies have also shown SDS to be more effective at removing DNA from decellularized tissues[8].

The device was designed because we found that whole sections of muscle took a considerable amount of time compared to other decellularized tissues. Merritt *et al.* discussed injecting muscles with SDS multiple times throughout the day in order to increase the rate of decellularization[10]. The injections were time consuming and require considerably more decellularization fluid. Our goal was to develop a device that could constantly deliver SDS to a muscle to shorten the time needed to achieve complete decellularization, while not negatively affecting the biochemical and morphological properties of decellularized muscle. Using a syringe pump to deliver SDS at known flow rates would enable us to compare flow rates and time to complete decellularization. In order to quantify the time to decellularization, the device would also need to be capable of real-time monitoring of decellularization progress.

The macroscopic characteristics of muscle and decellularized muscle were used to design the monitoring component of this device. Muscle is opaque and pinkish red in color while decellularized muscle is much more transparent and white in color. Myoglobin, an oxygen-binding protein found within muscle cells, is responsible for the pinkish red color seen in intact muscle. As cells are lysed by SDS, the myoglobin is flushed out of the remaining ECM along with other intracellular molecules. As the tissue approaches complete decellularization, the amount myoglobin and other molecules that absorb light reaches a minimum. Once all cellular components are removed, the

3

macroscopic and optical properties of the decellularized muscle remain constant and the tissue can be assumed to be decellularized. Characterization of the perfusion decellularized muscle with fluorescent labelling was used to validate claims of complete decellularization. Biochemical assays were performed to quantify and compare the ECM produced by the device to ECM derived through current decellularization protocols.

METHODS

Spectral Properties of Skeletal Muscle

An absorbance spectral sweep was performed on rat (Sprague Dawley) gastrocnemius muscle samples in order to characterize the optical properties of native and decellularized skeletal muscle. The gastrocnemius muscle was selected based on its past use in muscle regeneration animal studies; the anticipated area of application for this device. All animals used in this study were previously sacrificed as part of an unrelated study and stored at -20°C until required for testing. In preparation for testing, gastrocnemius muscle samples were dissected, and from each whole muscle sample a central core was harvested using a biopsy punch (diameter = 6mm) and trimmed to a thickness of 4mm. Cylindrical muscle sample cores were loaded into 96 well plates (one sample per well) and incubated in a 1% SDS solution for 24 and 48 hours at room temperature following published protocols. Untreated muscle samples were maintained as controls (n=3 / sample group). At the prescribed time points, a spectral sweep of tissue sample absorbance was measured (400-900nm, step size = 5nm) with the aid of a plate reader (Biotek Model, Winooski, VT). For comparison, the absorbance spectra of

myoglobin, an abundant intracellular skeletal muscle protein, were also characterized

(0.1, 0.3, and 0.6% in phosphate buffered saline). Absorbance versus wavelength data

for all muscle and myoglobin samples were plotted and examined for the presence of

decellularization sensitive absorbance peaks

Device Design and Fabrication

The design goal was to combine continuous tissue perfusion and real time optical

monitoring into a single bench top decellularization device. The two primary

components of the device are the muscle perfusion units and optical detection collars

with integrated data collection hardware and software. The perfusion units, optical

monitoring collars, and data collection hardware are housed within and mounted onto a

custom fabricated two piece enclosure (**Figure 1**). The enclosure was designed to

accommodate four individual decellularization units each capable of accommodating a

single muscle tissue sample. The closure also isolates the optical monitoring collars

from ambient light. Each of the four modular perfusion units consists of a rigid acrylic

cylinder (ID = 10mm; length = 40mm) which form the translucent perfusion chamber.

The inlet and outlet of each chamber is enclosed by watertight ports fashioned with Leur

lock style fitting and fabricated in acrylic with the aid of a 3-D printer (Objet 30, Objet,

Israel). The inlet port incorporates a removable 26-ga stainless steel hypodermic needle

(length = 20 mm). The needle is used to deliver decellularization solution deep into the

interior of individual muscle samples (**Figure 2**). The flow of decellularization fluid into

each decellularization unit was controlled via a commerical syringe pump (Model 210,

Harvard Apparatus, Holliston, MA) capable of delivering fluid to all four chambers over a

broad range of flow rates (0.1 to 10ml/hr) that would be evaluated during device characterization. Waste decellularization solution is collected in a reservoir for disposal or evaluation.

The optical collar was fitted with a single light emitting diode (LED) producing a peak emmitance centered at 535nm. Peak LED wavelength selection was motivated by the results of the previously described muscle optical property characterization. The light output of the LED is directed across the diameter of the collar. Located opposite to the LED emitter, is a light dependent resistor (LDR) detector. The LDR detector converts light intensity in photons to resistance in ohms. The optical collar with integrated LED and LDR can be positioned along the length of the decellularization unit. During decellularization monitoring the collar is positioned over the muscle sample, such that the muscle tissue impedes the light path from the LED emitter to the LDR detector. Analog voltages collected from the LDR were converted to digital values using a 16-bit analog-to-digital converter (ADC) (Adafruit, NYC, NY). A miniaturized single board computer (Raspberry Pi Foundation, United Kingdom) was used to power the LEDs and to control collection of the digitized LDR voltage signal from the ADC. Custom designed software (Python) was created to collect the voltage data and log it to an online spreadsheet. Optical data was collected from the LDR every five minutes. The complete system, including syringe pump and flat screen monitor, occupies a 0.5m X 0.5m footprint, a space that is compatible with typical laboratory workbenches.

<u>Perfusion Decellularized Muscle Characterization</u>

For all device characterization testing, medical gastrocnemius muscle tissue was harvested from Sprague Dawley rats and stored at -80°C until needed for testing as previously described. Prior to decellularization all muscles were thawed and rinsed briefly in DI water to remove any superficial blood or loosely adhered tissue. Whole muscle samples were loaded into perfusion chambers, one muscle per chamber, and the position was adjusted until the needle tip was visually located at the mid-belly region of the muscle. Based on static decellularization pilot testing and guided by published methods, muscle samples were perfused using a 1% SDS solution for a duration of 24 hours at a flow rate of 1ml/hr. Samples (n=4/timepoint) were collected both midway through and at the completion of the perfusion treatment. Untreated muscle samples were maintained as controls.

To explore the influence of key perfusion parameters (flow rate and solution concentration) on decellularization duration, medial gastrocnemius muscle samples were perfused at flow rates of either 0.1, 1, and 10mL/hr using SDS solutions at concentration of 0.2 and 1%. A total of 6 parameter combinations were explored (n= 4/ parameter condition). Throughout perfusion testing the optical properties of each muscle was measured and digitally logged every 5 minutes. The time to sample decellularization was recorded as the time at which sample optical properties were unchanged (<0.1% difference from the previous recording) for five continuous recording (25 minutes). Histological data will be used to validate that tissues are decellularized at

this endpoint. For comparison, statically decellularized muscle samples were maintained as controls.

To examine the relationship between muscle optical properties and histological appearance, representative untreated control and perfusion treated samples were embedded in tissue freezing media (Triangle Biomedical Sciences, Inc., Durham NC), sectioned at 8μm with a cryostat, and mounted onto glass microscope slides. Perfused treated samples were selected from either the endpoint on the To visualize intracellular proteins, mounted sections were immunoreacted for the presence of myoglobin (αrat myoglobin, rabbit IgG1, 500:1, Sigma, St. Lous MO) and actin (phalloidin, 40:1, Sigma, St. Louis MO) followed by incubation with the appropriate fluorescently labeled secondary antibodies (αIgG, 500:1, Invitrogen, Carlsbad, CA). Sections were counterstained with the nuclear staining reagent DAPI, and then microscopically imaged (Ci-L, Nikon, Troy, NY). Digital images were captured, stored, and examined for the presence of intracellular proteins and nuclear remnants.

To determine whether perfusion decellularization influenced the retention of key ECM molecules within treated muscle samples the sulfated glycosaminoglycans (sGAG) content for control and perfusion samples was quantified using the procedure detailed in Barbosa *et al*[21]. Briefly, decellularized muscle samples (control and perfusion) were digested in a solution containing 50 μg/mL proteinase K in 100 mM K_2HPO_4 at a pH of 8.0 at 55ºC for 16 hours. The samples were then centrifuged and filtered to obtain an extract free of tissue fragments. A 1,9-dimethylmethylene blue (DMMB) solution was added to produce an insoluble GAG-DMMB complex. The solution was then centrifuged and the supernatant was removed and the GAG-DMMB

complex was dissolved with a decomplexation solution. The absorbance of the resulting

solution was read at 656 nm with the aid of a plate reader (BioTek, Winooski, VT).

The collagen content for the control and perfusion samples was quantified using

a hydroxyproline assay. A modified version of the procedure found in Edwards was

used to analyze collagen content[22]. Briefly, all tissue samples were hydrolyzed in 6N

HCl for 16-20 hours at 115ºC. After which, samples were cooled to RT and diluted 1:5 in

DI water. A buffer composed of citric acid monohydrate, glacial acetic acid, sodium

acetate, sodium hydroxide, 1-propanol and toluene was prepared according to

Edwards. Hydroxyproline was dissolved in 100mL of the buffer at this stage to produce

a hydroxyproline standard. Chloramine-T was dissolved in DI water and in addition to 1-

propanol, was added to the buffer. A second buffer composed of 4-

dimethylaminobenzaldehyde, 1-propanol, and perchloric acid was also prepared. A

standard dilution was prepared in a 96-well plate and 50 µL of each sample was added

in triplicate. 100 µL of each buffer was added to each well (samples and standards) and

the plate was read immediately at 570 nm with the aid of a plate reader (BioTek,

Winooksi, VT).

RESULTS

Spectral Characterization of Skeletal Muscle

The absorbance spectral sweep for myoglobin solutions show a decreasing

absorbance peak with lower concentrations of myoglobin (**Figure 4A**). The absorbance

peak is found between 480-550 nm in the 0.6% solution. The absorbance peak of the

0.3% myoglobin solution is 58% smaller than the 0.6% solution. The 0.1% solution has

an absorbance peak that is 85% smaller than the 0.6% myoglobin solution.

Decellularizing skeletal muscle in 96-well plates provided quantitative data on the

progress of decellularization in the form of absorbance spectra. A representative sample

of the absorbance spectra of rat skeletal muscle, partially decellularized muscle and

decellularized muscle is shown in **Figure 4B**. An absorbance peak appears around 520-

550 nm in the muscle sample, is present but less pronounced in PDM and absent in

decellularized muscle**.** The absorbance peak for the PDM is 37% smaller than the

absorbance peak of the untreated muscle. Although there appears to be a peak under

450 nm, the plate reader was unable to produce reliable absorbance data at such small

wavelengths.

Device Design and Fabrication

The device performed as designed and produced decellularized muscle samples

for multiple flow rates and SDS concentrations. Four decellularization chambers were

housed in the 3D printed box (**Figure 3A**). The Raspberry Pi microcomputer, ADC,

GPIO breakout board, and a custom PCB were all mounted to the 3D printed top

(**Figure 3B**). The complete assembly of the device was connected to the internet, an

LCD monitor, and a keyboard and then powered through the Raspberry Pi (**Figure 3: C**

& D). The Raspberry Pi with the ADC was sufficient for monitoring the voltage of the

LDR and the python program was able to reliably upload the data to a log file saved in

Google spreadsheets. The log file, which could be read in real-time or after the

completion of decellularization, provided meaningful data on the decellularization progress of four chambers simultaneously.

Perfusion Decellularized Muscle Characterization

The cryosectioned and stained native skeletal muscle tissue samples showed the presence of myoglobin, actin and nuclear remnants (**Figure 5:A & D**) and myofiber alignment (**Figure 5A**). Although nuclear remnants cannot be seen in the midpoint decellularized muscle samples, myoglobin and intracellular actin can still be detected (**Figure 5:B & E**). Endpoint decellularized muscle tissue displayed an absence of myoglobin, intracellular actin, and nuclear remnants (**Figure 5:C & F**). Individual myofibers can be seen in **Figure 5:A & D**, however, after partial decellularization the intact myofibers are absent in **Figures 5:B & E**.

The voltage logs generated by the Python program (**Figure 6**) provide a visualization of decellularization progress. Muscles were determined to be completely decellularized when the previous 5 readings had less than 0.1% change. The control sample was not included; After one week, the muscle was not completely decellularized. At an SDS concentration of 0.2%, the hours to decellularization were 142.7 ± 7.7, 42.4 ± 3.0, 9.9 ± 1.2 for the flow rates of 0.1 mL/hr, 1.0 mL/hr, and 10 mL/hr respectively. While at an SDS concentration of 1.0%, the hours to decellularization were 107.0 ± 6.5, 35.1 ± 2.5, 7.2 ± 1.0 for the flow rates of 0.1 mL/hr, 1.0 mL/hr, and 10 mL/hr

respectively. Although SDS concentration did have a significant effect on time to decellularization (**Figure 7**), the device flow rate had a much greater effect.

Perfusion decellularization did not significantly affect collagen or sGAG concentration when compared to diffusion decellularized control samples. Regardless of flow rate or SDS concentration, none of the samples had significant differences in either collagen or sGAG from the control samples (**Figure 8**). All averages were within 10% of the diffusion decellularized control samples and of each other. No trends were observed with regard to flow rate or concentration.

DISCUSSION

This device was primarily developed to decellularize bulky pieces of skeletal muscle which are to be used as a template for engineered ECM scaffolds that are being created in our lab[23]. In order to speed up decellularization of bulk skeletal muscle, Merritt et al. injected muscle with SDS several times[10]. We found that bulky skeletal muscle, such as MGAS, were not decellularized after up to a week in SDS simply with agitation and daily solution changes. The purpose of this device was to provide constant injection of SDS into the muscle to increase the rate of decellularization and to reduce the amount of man-hours needed for injecting and changing solutions. The placement of the needle into the midbelly of the muscle had a great effect on the time to complete decellularization and practice was required to achieve consistent positioning and results. The time to complete decellularization was greatly decreased by forcing SDS out from the inside of the muscle rather than simple diffusion of SDS from the outside of the muscle.

In addition to decreasing the time to decellularization, this device is also able to monitor the progress of decellularization. The macroscopic characteristics of muscle and decellularized muscle were used to design the monitoring component. Rat skeletal muscle is opaque and pink-red in color while decellularized muscle is much more transparent and white in color. By decellularizing muscle in a 96-well plate and obtaining an absorbance spectral sweep, we were able to quantify the change from muscle to acellular ECM. We observed a local absorbance peak in the 520-550nm range in muscle that was not seen in the decellularized muscle and was much less prominent but still visible in the partially decellularized muscle (Figure 4). Although the actual absorbance value was dependent on the thickness of the tissue, the local peak was present in all muscle samples and absent in all decellularized samples. An LED with a wavelength of 535 nm was selected for the detection collar to take advantage of the absorbance peak. The muscle would therefore absorb less light as decellularization progressed. In turn, as more light was transmitted through the tissue, the voltage across the LDR would decrease. When the tissue had been completely decellularized, the voltage across the LDR changed very little from one reading to the next. When five consecutive voltage readings had less than 0.1% change, the sample was considered to be decellularized.

The concentrations of SDS used to test the decellularization device were 1%, as is seen in many SDS decellularization protocols, and 0.2%. The lower concentration was used as it is below the critical micelle concentration (CMC) for SDS, ~0.225%[24]. The concentration of SDS had a significant effect on the time to decellularization but the flow rate had a much larger effect (Figure 7). Although SDS-based protocols have been

found to cause significant deterioration of the ECM compared to other detergents and decellularization protocols[8,25,26], SDS was chosen for this device as it provided a simple protocol and has been used in other perfusion based decellularization methods. Collagen and sGAG were quantified for all the conditions to determine if perfusion based decellularization had a deleterious effect on the acellular ECM. Any advantages the perfusion device could provide would be for naught if the system produced substandard scaffolds. The biochemical composition of the ECM from the perfused and control samples did not differ significantly from one another (Figure 8).

The detection collar and associated hardware and software allowed us to monitor in real-time the progress of the tissue from muscle to acellular ECM. The device was originally tested using a desktop computer and National Instruments LabView software to log the voltage data from the LDRs. While the device was fully functional and performed as designed, the device neither required the computing power of the desktop computer nor the robustness of the LabView software package. The Raspberry Pi provides internet connectivity, a platform for programming in Python, and a set of GPIO pins, all of which were used in this application and allowed the device to operate as a stand-alone device. Once the device was set up and connected to the internet using an Ethernet cord, the device did not need a monitor, mouse or keyboard as it could be accessed using SSH protocol. In addition to starting via the command line, the python program could be initiated and shutdown with an SSH client from any smartphone or desktop computer with internet connectivity. Logging the voltage data every five minutes was sufficient for analyzing decellularization progress without creating an extremely large file.

14

This device is novel in its approach to decellularize skeletal muscle and to monitor the progress of decellularization. However, there is not a widespread need for the ECM processed by this device. Most regenerative medicine strategies for skeletal muscle repair involve very thin (<3mm) acellular scaffolds, as host cells do not infiltrate much further than that when used to repair skeletal muscle in vivo. Host cell infiltration is dependent on angiogenesis within the implanted scaffold[6]. Even with established or nascent vasculature in vitro, without immediate anastomosis with the host's vasculature, cells in the interior of a scaffold will not survive. Until progress is made toward angiogenesis and/or revascularization of tissue constructs post-implantation, bulky skeletal muscle ECM will not have a translational application.

Potential refinements to the device include controlling the syringe pump with the Raspberry Pi, along with modifications to the enclosure to improve loading of muscles into the chambers and to increase the number of chambers that can be housed. If the production of acellular ECM needs to be increased, the device can be expanded. The device was designed to be modular in that a single chamber could be used or up to four chambers, using the current housing, could be run simultaneously. Although the number of chambers is limited by the capacity of our current syringe pump, the Raspberry Pi and ADC can accommodate eight analog voltage inputs. In addition, other decellularization protocols could be adapted for use in this device. Another use for this device could also be to recellularize acellular scaffolds by flowing media into the midbelly of the scaffold. This would require a much faster flow rates, a peristaltic pump instead of a syringe pump, and a separate reservoir for gas exchange within the media. Additionally, the device would have to operate in an incubator under sterile conditions.

Preliminary trials have begun adapting other decellularization solutions and protocols for use in this perfusion driven device. In addition, this device is currently being operated to provide skeletal muscle ECM scaffolds which are being used to study the repair of VML in a rat model. The perfusion derived skeletal muscle ECM is part of a larger investigation into VML repair including comparisons to cell-derived ECM as a biologic tissue repair scaffold.

FIGURES
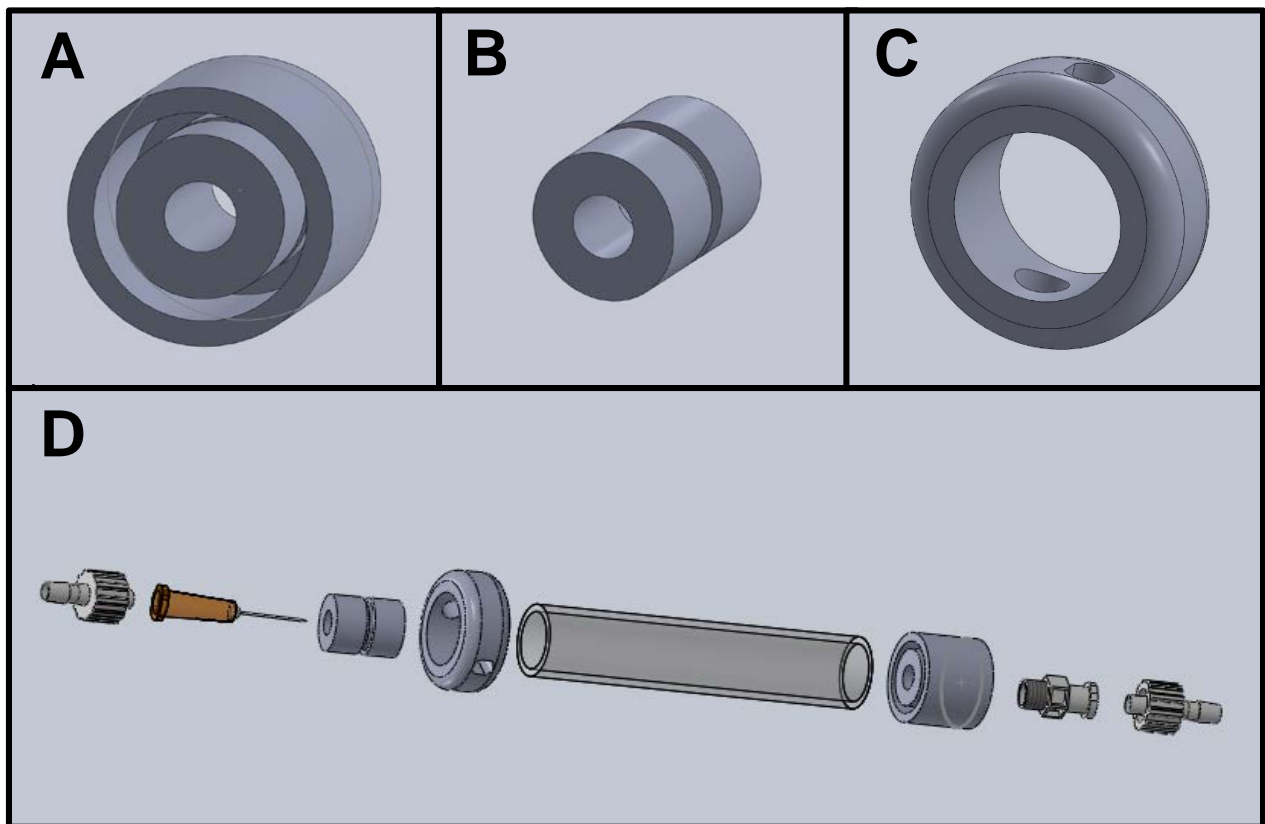
Figure 1: A-C Components of the decellularization chamber as drawn in SolidWorks and printed on a 3-D Printer. A. Outlet port. B Inlet port. C Detection collar. D Decellularization chamber as designed in SolidWorks, complete with Leur lock connectors and 26 ga. needle.
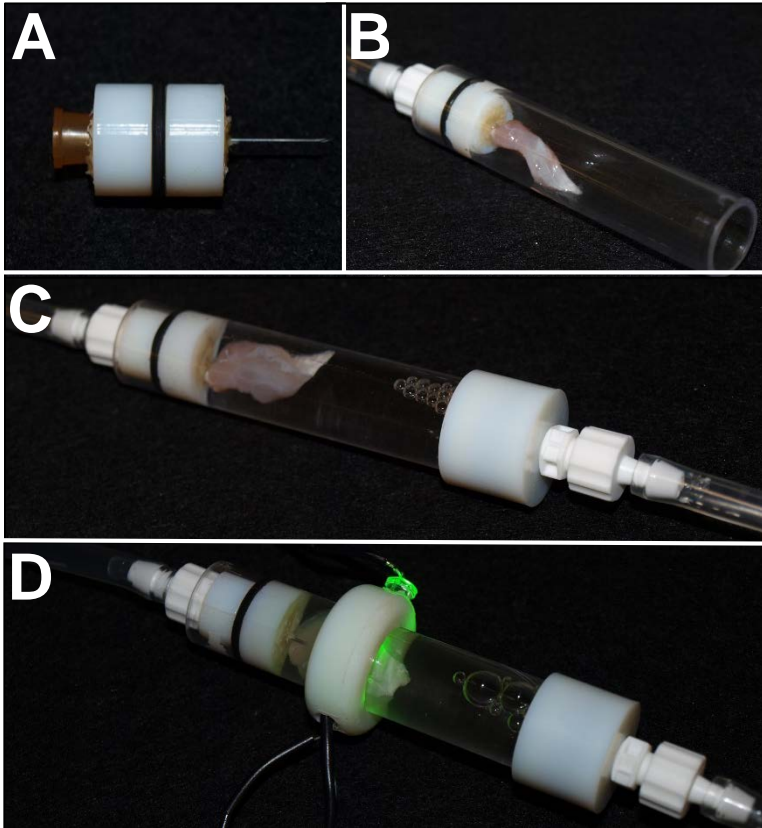
Figure 2: A. 26 ga. needle epoxyed into inlet port. B. Inlet is connected to syringe pump and needle is inserted in muscle. C. Chamber is filled with SDS and outlet is connected to waste collector. D. Detector is positioned around the muscle. (Photos by Benjamin Kasukonis)
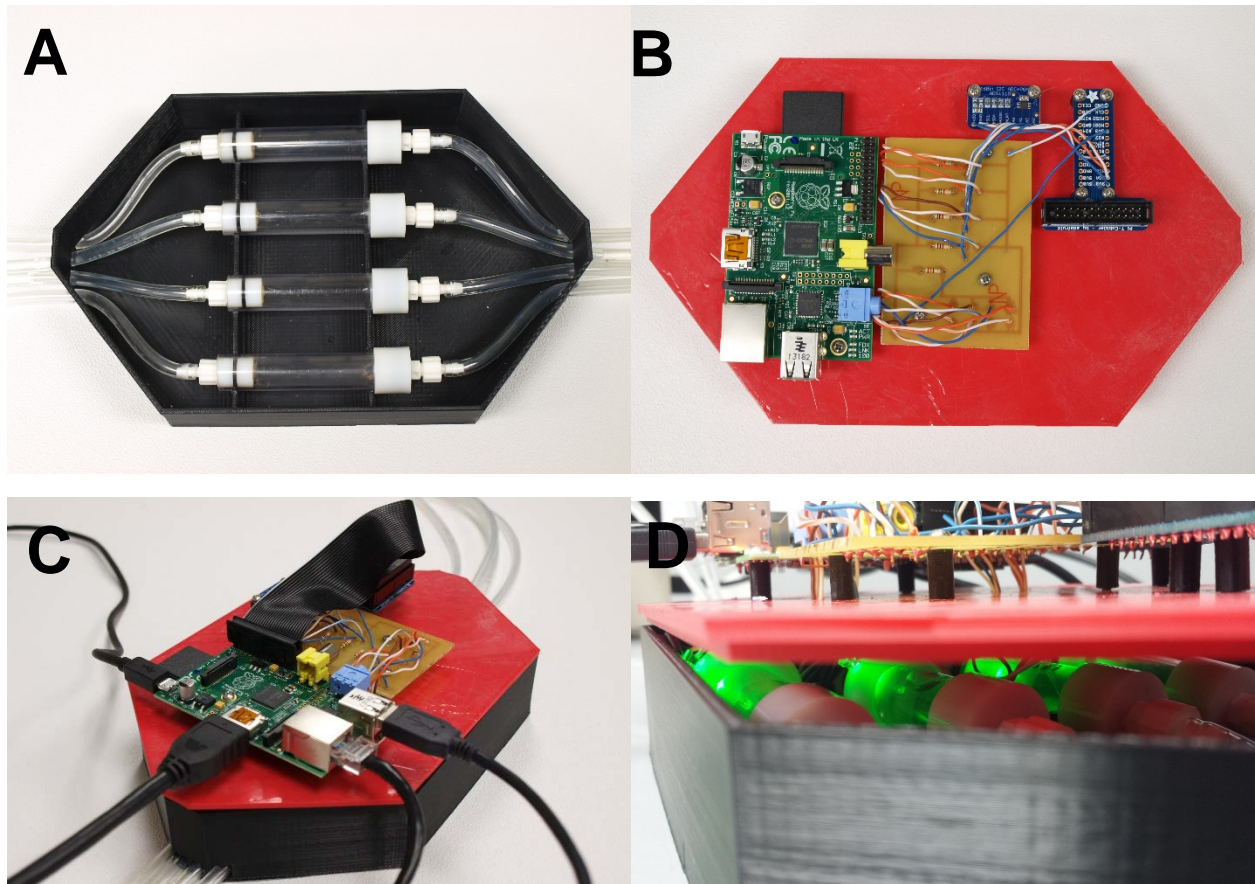
Figure 3: A. Four decellularization chambers inserted in the lower portion of the device. B. Top of the device with the Raspberry Pi, ADC, circuit board, and GPIO breakout C. Complete assembly of the decellularization device. D. Inside view of the device. (Photos by Benjamin Kasukonis
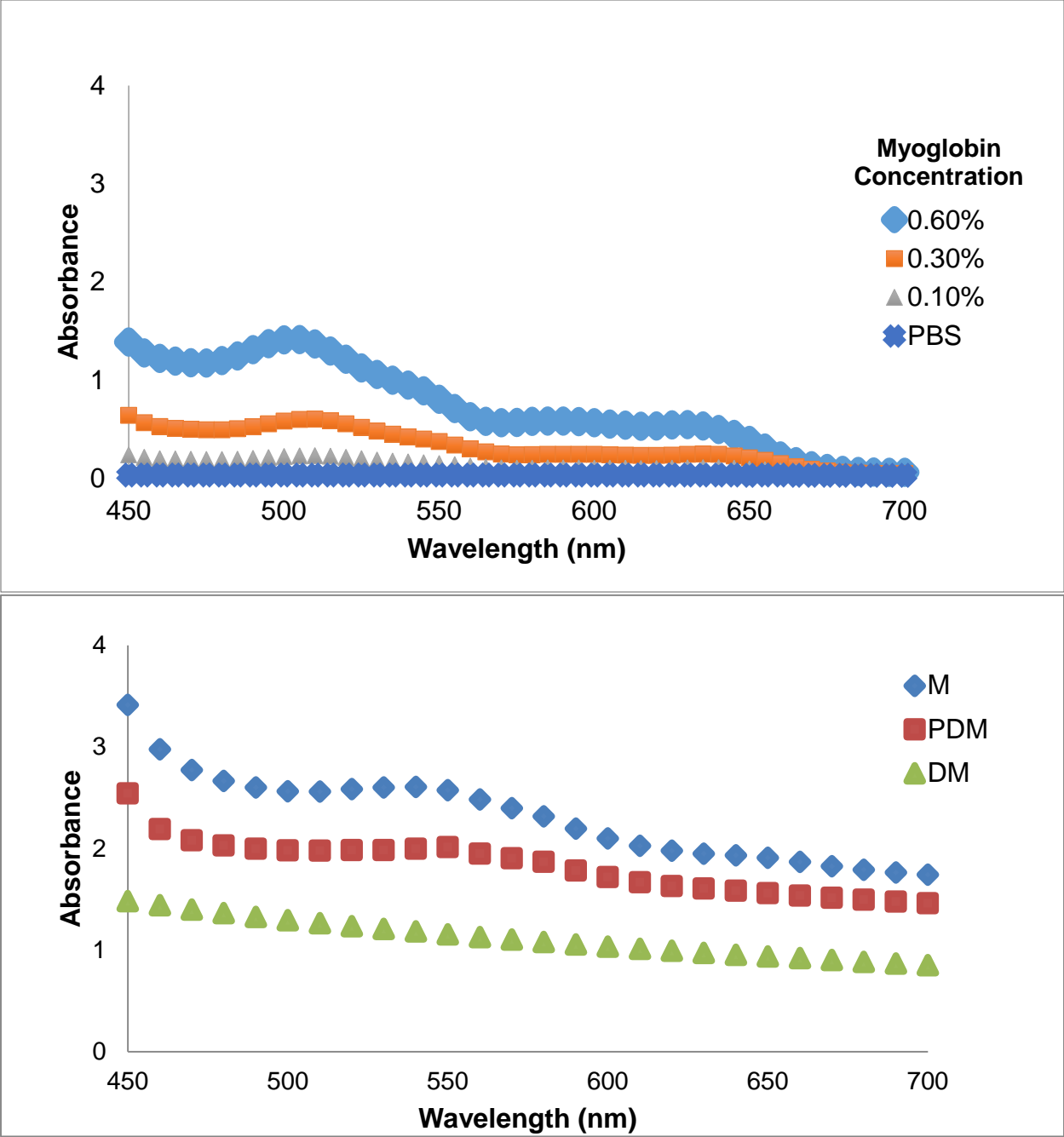
Figure 4: A. Absorbance spectra for various concentrations of myoglobin. B. Absorbance spectra for representative samples of muscle (M), partially decellularized muscle (PDM), and decellularized muscle (DM).
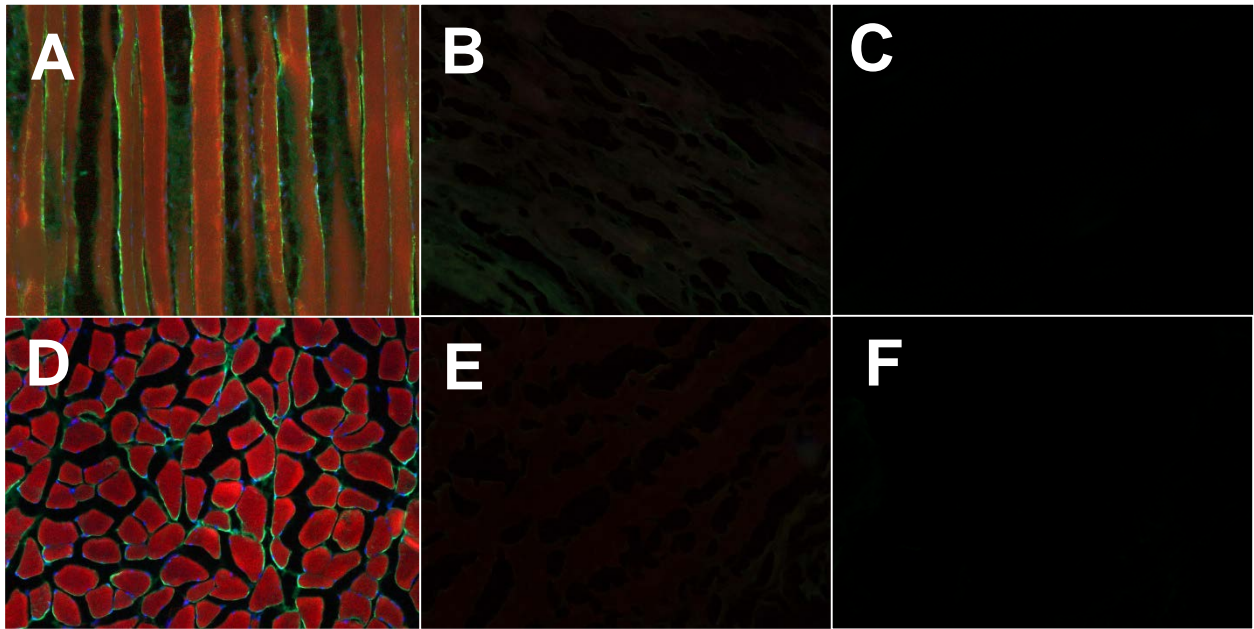
Figure 5: 8μm muscle(A,D), midpoint perfusion decellularized muscle(B,E), and endpoint perfusion decellularized muscle(C,F) sections stained with phalloidin(red), DAPI(blue), and immunostained for myoglobin(green). A-C Longitudinal sections. D-F Transverse sections. (Images by Benjamin Kasukonis)
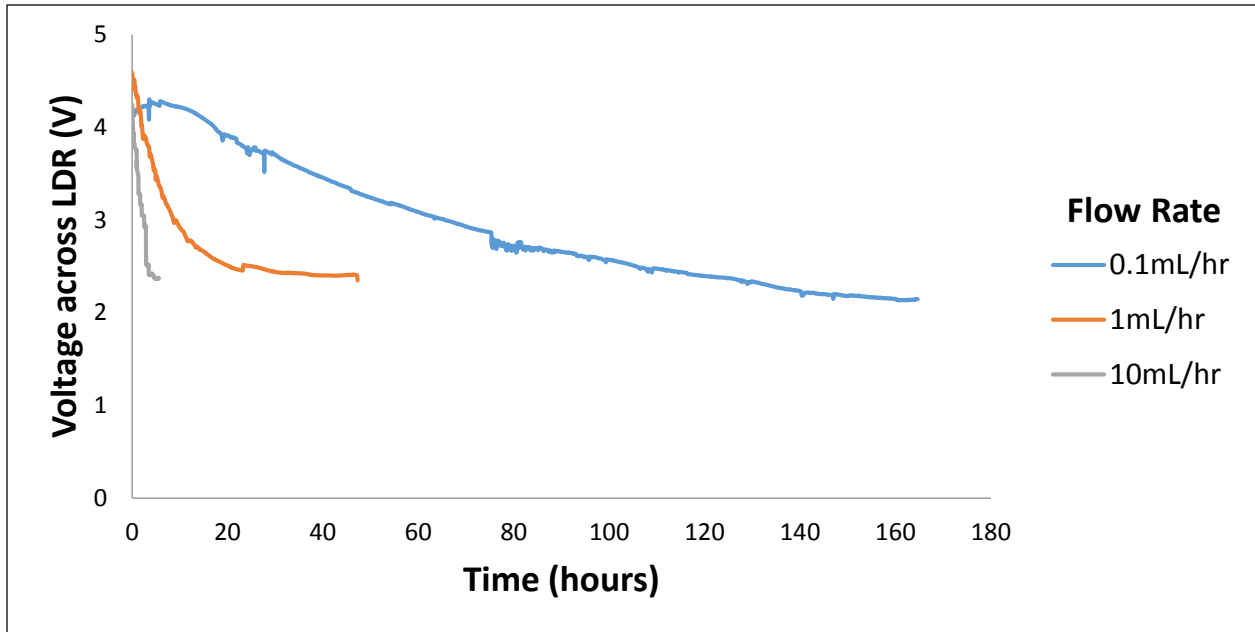
*Figure 6: Representitive voltage logs displaying decellularization progress from 0.2%
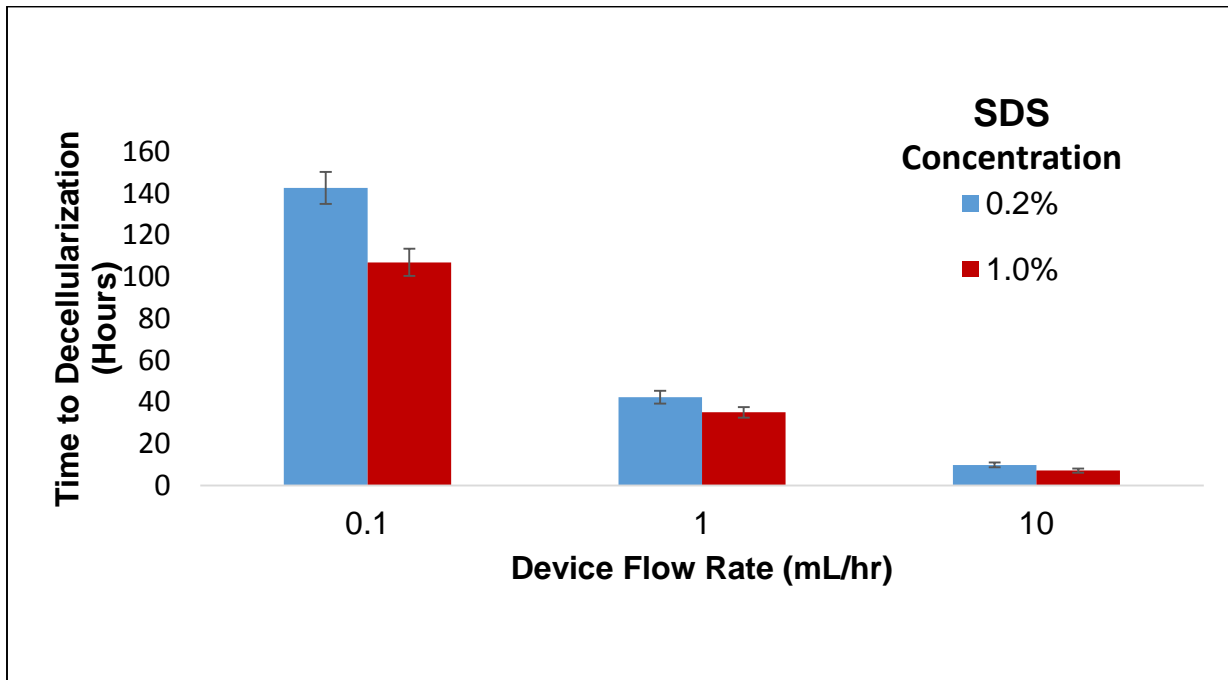SDS perfused samples.*

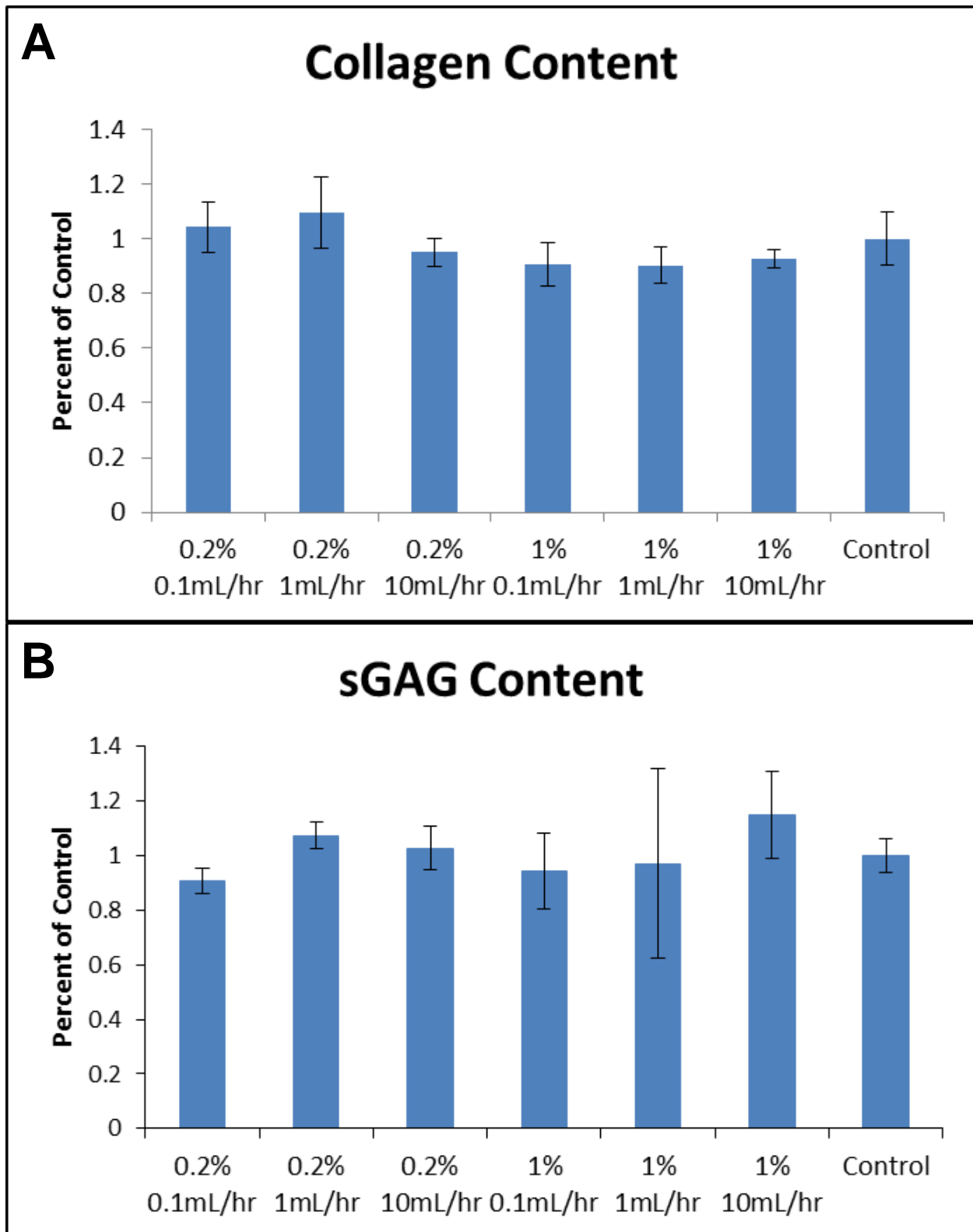*Figure 7: Comparison of SDS concentrations and device flow rates. n=4 for all
conditions.*

Figure 8: A. Collagen content as measured by hydroxyproline assay. B. sGAG content as measured by DMMB assay. n=4 for all groups.

REFERENCES

1. Borschel, G.H., Dennis, R.G., and Kuzon, W.M.J. Contractile Skeletal Muscle Tissue-Engineered on an Acellular Scaffold. Plastic and Reconstructive Surgery **113**, 2004.

2. Bi, H., and Jin, Y. Current progress of skin tissue engineering: Seed cells, bioscaffolds, and construction strategies. Burns and Trauma **1**, 63, 2013.

3. Fisher, M.B., and Mauck, R.L. Tissue engineering and regenerative medicine: recent innovations and the transition to translation. Tissue Engineering Part B: Reviews **19**, 1, 2013.

4. Jayarama Reddy, V., Radhakrishnan, S., Ravichandran, R., Mukherjee, S., Balamurugan, R., Sundarrajan, S., and Ramakrishna, S. Nanofibrous structured biomimetic strategies for skin tissue regeneration. Wound Repair and Regeneration **21**, 1, 2013.

5. Juhas, M., Engelmayr, G.C.,Jr, Fontanella, A.N., Palmer, G.M., and Bursac, N. Biomimetic engineered muscle with capacity for vascular integration and functional maturation in vivo. Proceedings of the National Academy of Sciences of the United States of America **111**, 5508, 2014.

6. Turner, N.J., and Badylak, S.F. Regeneration of skeletal muscle. Cell and tissue research **347**, 759, 2012.

7. Corona, B.T., Ward, C.L., Baker, H.B., Walters, T.J., and Christ, G.J. Implantation of in vitro tissue engineered muscle repair constructs and bladder acellular matrices partially restore in vivo skeletal muscle function in a rat model of volumetric muscle loss injury. Tissue Engineering Part A **20**, 705, 2013.

8. Gillies, A.R., Smith, L.R., Lieber, R.L., and Varghese, S. Method for decellularizing skeletal muscle without detergents or proteolytic enzymes. Tissue Engineering Part C: Methods **17**, 383, 2010.

9. Hinds, S., Bian, W., Dennis, R.G., and Bursac, N. The role of extracellular matrix composition in structure and function of bioengineered skeletal muscle. Biomaterials **32**, 3575, 2011.

10. Merritt, E.K., Cannon, M.V., Hammers, D.W., Le, L.N., Gokhale, R., Sarathy, A., Song, T.J., Tierney, M.T., Suggs, L.J., Walters, T.J., and Farrar, R.P. Repair of traumatic skeletal muscle injury with bone-marrow-derived mesenchymal stem cells seeded on extracellular matrix. Tissue Engineering.Part A **16**, 2871, 2010.

11. Perniconi, B., Costa, A., Aulino, P., Teodori, L., Adamo, S., and Coletti, D. The pro-myogenic environment provided by whole organ scale acellular scaffolds from skeletal muscle. Biomaterials **32**, 7870, 2011.

12. Valentin, J.E., Turner, N.J., Gilbert, T.W., and Badylak, S.F. Functional skeletal muscle formation with a biologic scaffold. Biomaterials **31**, 7475, 2010.

13. Wang, L., Johnson, J.A., Chang, D.W., and Zhang, Q. Decellularized musculofascial extracellular matrix for tissue engineering. Biomaterials **34**, 2641, 2013.

14. Wolf, M.T., Daly, K.A., Reing, J.E., and Badylak, S.F. Biologic scaffold composed of skeletal muscle extracellular matrix. Biomaterials **33**, 2916, 2012.

15. Gilbert, T.W., Sellaro, T.L., and Badylak, S.F. Decellularization of tissues and organs. Biomaterials **27**, 3675, 2006.

16. Ott, H.C., Matthiesen, T.S., Goh, S., Black, L.D., Kren, S.M., Netoff, T.I., and Taylor, D.A. Perfusion-decellularized matrix: using nature's platform to engineer a bioartificial heart. Nature medicine **14**, 213, 2008.

17. Uygun, B.E., Soto-Gutierrez, A., Yagi, H., Izamis, M., Guzzardi, M.A., Shulman, C., Milwid, J., Kobayashi, N., Tilles, A., and Berthiaume, F. Organ reengineering through development of a transplantable recellularized liver graft using decellularized liver matrix. Nature medicine **16**, 814, 2010.

18. Ott, H.C., Clippinger, B., Conrad, C., Schuetz, C., Pomerantseva, I., Ikonomou, L., Kotton, D., and Vacanti, J.P. Regeneration and orthotopic transplantation of a bioartificial lung. Nature medicine **16**, 927, 2010.

19. Sullivan, D.C., Mirmalek-Sani, S., Deegan, D.B., Baptista, P.M., Aboushwareb, T., Atala, A., and Yoo, J.J. Decellularization methods of porcine kidneys for whole organ engineering using a high-throughput system. Biomaterials **33**, 7756, 2012.

20. Levenberg, S., Rouwkema, J., Macdonald, M., Garfein, E.S., Kohane, D.S., Darland, D.C., Marini, R., van Blitterswijk, C.A., Mulligan, R.C., and D'Amore, P.A. Engineering vascularized skeletal muscle tissue. Nature biotechnology **23**, 879, 2005.

21. Barbosa, I., Garcia, S., Barbier-Chassefiere, V., Caruelle, J.P., Martelly, I., and Papy-Garcia, D. Improved and simple micro assay for sulfated glycosaminoglycans quantification in biological extracts and its use in skin and muscle tissue studies. Glycobiology **13**, 647, 2003.

22. Edwards, C. Modified assay for determination of hydroxyproline in a tissue hydrolyzate. Clinica chimica acta **104**, 161, 1980.

23. Wolchok, J.C., and Tresco, P.A. The isolation of cell derived extracellular matrix constructs using sacrificial open-cell foams. Biomaterials **31**, 9595, 2010.

24. Dominguez, A., Fernandez, A., Gonzalez, N., Iglesias, E., and Montenegro, L. Determination of Critical Micelle Concentration of Some Surfactants by Three Techniques. Journal of chemical education **74**, 1227, 1997.

25. Faulk, D.M., Carruthers, C.A., Warner, H.J., Kramer, C.R., Reing, J.E., Zhang, L., D'Amore, A., and Badylak, S.F. The effect of detergents on the basement membrane complex of a biologic scaffold material. Acta biomaterialia **10**, 183, 2014.

26. Keane, T.J., Londono, R., Turner, N.J., and Badylak, S.F. Consequences of ineffective decellularization of biologic scaffolds on the host response. Biomaterials **33**, 1771, 2012.

APPENDIX:

Python program

```python
#!/usr/bin/python

import time, signal, sys, datetime, gspread
from Adafruit_ADS1x15 import ADS1x15

#Function from signal library that will end script (Ctrl+C)
def signal_handler(signal, frame):
        print 'Session Ended'
        sys.exit(0)
signal.signal(signal.SIGINT, signal_handler)


ADS1015 = 0x00  # 12-bit ADC
ADS1115 = 0x01    # 16-bit ADC

# Select the gain
# gain = 61    # +/- 6.144V
gain = 4096  # +/- 4.096V
# gain = 2048  # +/- 2.048V
# gain = 1024  # +/- 1.024V
# gain = 512   # +/- 0.512V
# gain = 256   # +/- 0.256V

# Select the sample rate
sps = 8     # 8 samples per second
# sps = 16   # 16 samples per second
# sps = 32   # 32 samples per second
# sps = 64   # 64 samples per second
# sps = 128  # 128 samples per second
# sps = 250  # 250 samples per second
# sps = 475  # 475 samples per second
# sps = 860  # 860 samples per second

# Initialize the ADC using the default mode (use default I2C address)
adc = ADS1x15(ic=ADS1115)

# Read voltage in single-ended mode using ADS1x15 library
# volts = adc.readADCSingleEnded(channel, gain, sps) / 1000
# Example: To read channel 3 in single-ended mode, +/- 1.024V, 860 sps use:
# volts = adc.readADCSingleEnded(3, 1024, 860)


# Define the functions that will be used to query the ADC for voltage
def read1():

      volts1 = adc.readADCSingleEnded(0, gain, sps) / 1000

      return volts1

def read2():

      volts2 = adc.readADCSingleEnded(1, gain, sps) / 1000
```

```python
        return volts2

def read3():

        volts3 = adc.readADCSingleEnded(2, gain, sps) / 1000

        return volts3

def read4():

        volts4 = adc.readADCSingleEnded(3, gain, sps) / 1000

        return volts4

print 'Checking account...'
#Google account details (Redacted for publication)
email = '******************'
password = '*********'




#Attempt to log in to google account using supplied credentials
try:
    gc = gspread.login(email,password)
except:
    print('Login information invalid.')
    sys.exit()
print 'Account valid.\n'

#Name of the spreadsheet to be appended
spreadsheet = 'Decell_Log'

#Open the spreadsheet
worksheet = gc.open(spreadsheet).sheet1
print 'Spreadsheet is ready.'
print "Decellularization logging will begin shortly. To exit, press
'Ctrl+C'\n"



#While loop to read voltages across LDRs and write to the log file
while True:

#Run the read() function created earlier to write voltages to respective
variables
        volts1 = read1()
        volts2 = read2()
        volts3 = read3()
        volts4 = read4()

#Write to the chosen spreadsheet with a timestamp and voltages from the LDRs
try:
        values = [datetime.datetime.now(), volts1, volts2, volts3, volts4]
            worksheet.append_row(values)
        except:
            print "Unable to append data."
```

27

```
        sys.exit()

#Print values to the CLI
print datetime.datetime.now(), volts1, volts2, volts3, volts4

#Time delay before next loop iteration (in seconds)
time.sleep(300)
```